# A Realistic Model of Biphasic Calcium Transients in Electrically Nonexcitable Cells

A. Korngreen,* V. Gold'shtein,# and Z. Priel*

Departments of Chemistry* and Mathematics,# Ben-Gurion University of the Negev, Beer-Sheva 84105, Israel

ABSTRACT   In many electrically nonexcitable cells, the release of calcium from internal stores is followed by a much slower phase in which the intracellular calcium concentration decreases gradually to a sustained value higher than the concentration before stimulation. This elevated calcium plateau has been shown to be the result of calcium influx. The model presented in this work describes a system consisting of a cytoplasmic calcium store and a plasma membrane calcium channel, both excitable by a membrane receptor; a fast cytoplasmic calcium buffer; and calcium pumps in both the calcium store and cellular membranes. Inherent difficulties in the numerical evaluation of the model, caused by very large calcium fluxes across the store membrane, were overcome by analytically separating the fast processes of calcium release from the slower processes of calcium cycling across the plasma membrane. This enabled the simulation of realistic biphasic calcium transients similar to those observed experimentally. The model predicted 1) a strong correlation between the rate of calcium cycling across the plasma membrane and the rate of calcium decay; and 2) a dependence on the level of cell excitation of the maximum rise in cytoplasmic calcium concentration, the level of the elevated calcium plateau, and the rate of calcium decay. Using the model, we simulated the washout of agonist from the bathing solution and the depletion of the calcium store by a pharmacological agent (such as thapsigargin) under several experimental conditions.

## INTRODUCTION

Many cellular events are triggered by changes in the cytoplasmic concentration of calcium ions (Berridge, 1993). Calcium ions bind to many different cellular proteins, modifying their activity and consequently affecting the behavior of the entire cell. Elevation of the cytoplasmic calcium concentration ($[Ca^{2+}]_i$) is required for the proper function of the cell, yet, unlike with other second messengers, prolonged high $[Ca^{2+}]_i$ can lead to cell death. Therefore, a dynamic integrated system for the regulation of cytoplasmic calcium concentration at rest and after stimulation has evolved. The $[Ca^{2+}]_i$ at rest ($\sim$0.1 $\mu$M) is four orders of magnitude lower than the extracellular calcium concentration ($\sim$2000 $\mu$M). To sustain this enormous gradient, the cell actively extrudes calcium ions from the cytoplasm into the extracellular medium. Calcium ions flow down this concentration gradient through many types of calcium channels in the plasma membrane (Tsien and Tsien, 1990). These cations are also removed from the cytoplasm by sequestration in specialized intracellular storage compartments, where their concentration can reach that found in the external medium. These storage compartments also contain channels through which calcium ions enter the cytoplasm (Pozzan et al., 1994). Thus, during rest, calcium homeostasis in the cytoplasm is maintained by the counteraction of passive calcium entry into the cytoplasm, with active extrusion of calcium ions from the cytoplasm into the store and

the external solution. Activation of the cell leads to an increase in the conductance of calcium channels in both the cellular membrane and the membrane enclosing the calcium store, causing a rise in $[Ca^{2+}]_i$. This increase in $[Ca^{2+}]_i$ is moderated by the action of calcium buffers in the cytoplasm (Zhou and Neher, 1993; Berlin et al., 1994) and by the active extrusion of calcium into the calcium store and the external medium. Because of the highly dynamic nature of this integrated system, a spectrum of fast, slow, and oscillatory cytoplasmic calcium transients has been observed.

In electrically nonexcitable cells such as epithelia, the predominant second messenger responsible for calcium release from intracellular stores is inositol 1,4,5-trisphosphate ($IP_3$) (Berridge, 1993). Binding of an agonist to a membrane receptor induces the synthesis of this molecule from membrane lipids. This second messenger then induces the release of calcium from its storage organelles by activating a ligand-gated channel located on the organelle surface. After this initial rise in $[Ca^{2+}]_i$, a much slower phase is observed. The influx of calcium through the plasma membrane has been observed to increase over prolonged periods of time (Rasmussen and Rasmussen, 1990). The cellular mechanisms regulating this calcium influx vary between cell types. The influx may be induced by activation of a receptor-operated calcium channel (Benham and Tsien, 1987), a second messenger-regulated calcium channel (Lückhoff and Clapham, 1992), or a second messenger generated by the depletion of the calcium stores (Putney, 1990; Randriamampita and Tsien, 1993). It has been suggested that the increased calcium concentration in the vicinity of the plasma membrane is due to an increased influx of calcium while the remainder of the cytoplasm remains at a lower calcium concentration (Rasmussen and Rasmussen, 1990; Alkone and Rasmussen, 1988).

The physiological significance of this prolonged calcium influx is great. The cell utilizes this mechanism to retain a high level of activation without maintaining harmfully high cytoplasmic calcium concentrations. We have observed, in ciliary cells from rabbit tracheal epithelium stimulated by purinergic agonists, that the transient rise in the cytoplasmic calcium concentration decays to a stable $[Ca^{2+}]_i$ level higher than the level before stimulation. The physiological response of these cells, an increase in ciliary beat frequency after stimulation, remains high for the duration of the stimulus (Korngreen and Priel, 1994, 1996). The level of the elevated calcium plateau and the rate of $[Ca^{2+}]_i$ decay to that elevated level are sensitive to the concentration of the purinergic agonist. Moreover, reducing the flux of calcium into the cell from the extracellular medium by lowering the extracellular calcium concentration (Korngreen and Priel, 1996) or by calcium channel blockers (Korngreen and Priel, 1993) abolishes the elevated calcium plateau. Elevated $[Ca^{2+}]_i$ plateaus have also been observed in ciliary cells from frog palate (Tarasiuk et al., 1995; Alfahel et al., 1996; Levin et al., 1997) and human nasal epithelia (Korngreen and Priel, 1993). Prolonged cellular activation, induced by calcium influx, has also been observed for aldosterone and insulin secretion (Rasmussen and Rasmussen, 1990).

Elevated calcium plateaus may contain information on the duration and magnitude of the calcium influx responsible for the prolonged activation of the cell. The retrieval of this information is not trivial, because, in most cases, the calcium concentration is measured as an average over the whole cell. Although a great deal of theoretical work has been done describing cytoplasmic calcium oscillations, only very recently have nonoscillating calcium transients in electrically nonexcitable cells been investigated (Wiesner et al., 1996). Hence we set out to model mathematically the biphasic calcium transients to construct a tool that might help in the analysis of the biphasic calcium transients observed in ciliary cells. A model consisting of simplified basic elements of the cellular calcium signaling mechanism is proposed. Following an analytical treatment of the model, we were able to produce computer simulations of biphasic calcium transients similar to those observed in ciliary cells.

## THE MODEL

When the intracellular calcium concentration is measured from a single cell by a photomultiplier or from a population of cells by a spectrofluorimeter, the $[Ca^{2+}]_i$ measured is an average value. Under these conditions, areas of high calcium concentration in the cytoplasm (caused by either calcium discharge from intracellular stores or calcium influx from the external solution) are summed together with areas of low calcium concentration, yielding a distorted view of the system. An accurate description of this system really requires both spatial and temporal variables. However, the calcium signaling system is highly complex, consisting of many functional units expressed by different cells. To de-

scribe such a system accurately in electrically nonexcitable cells would require a prohibitive number of equations and parameters, which would make it almost impossible to analyze the system. Instead, we have chosen to create a simple, spatially uniform model incorporating the changes in the average $[Ca^{2+}]_i$, using the minimum number of calcium signaling system functional units needed to do so. This simple model, which can be successfully analyzed quantitatively, provides a solid cornerstone upon which to build more complex models.

As already mentioned, the processes involved in biphasic calcium transients are the release of calcium from intracellular calcium stores and a subsequent prolonged calcium influx across the plasma membrane. Therefore, our model contains 1) a plasma membrane with a calcium channel, and 2) an intracellular calcium store bounded by a membrane containing a calcium channel. These calcium channels permit free passage of calcium ions dependent only on the gradient of calcium across the membrane they are incorporated into. Hence the rate constants of calcium efflux and influx through the store channel can be set equal to each other ($k_1 = k_{-1}$, in Fig. 1). We have modeled the channel as a simple pore because we want as general a picture of biphasic calcium transients as possible. Such a simplification of the release mechanism from the calcium has been successfully applied in recent modeling of calcium oscillations in neurons (Friel, 1995). In addition to this simple pore, the calcium store membrane also contains a pump responsible for the calcium uptake from the cytoplasmic
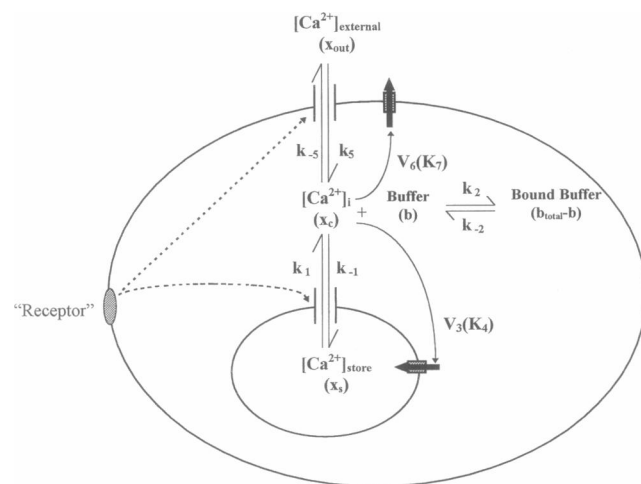


FIGURE 1   Schematic description of the dynamic model. Chemical equilibria are designated by solid arrows with appropriate rate constants written alongside. Variables are identified both by their names in the text and as mathematical symbols. Because the calcium channels in both the plasma membrane and the store membrane were modeled without preference to vectorial flow of the calcium, the arrows in the chemical equilibrium are bidirectional and the rate constants equal ($k_1 = k_{-1}$ and $k_5 = k_{-5}$). Activation of calcium channels in the calcium store and the plasma membrane is indicated by dotted arrows. Designation of the receptor in quotation marks is to denote the fact that the receptor was modeled as a linear activation term rather than as an agonist binding curve.

compartment into the store. The rate of calcium pumping has been set to depend on the cytoplasmic calcium concentration according to the Hill equation. The calcium channel in the plasma membrane has been modeled in a manner similar to that of the store channel, with the rate constants of calcium influx and efflux assumed to be equal ($k_5 = k_{-5}$). Although the calcium channels in both the plasma and calcium store membranes have been defined as bidirectional pores with equal rate constants in both directions, the cytoplasmic calcium concentration is always much smaller than the calcium concentration in either the external solution or the calcium store, so the actual rate of calcium passage through these channels against the chemical gradient is negligible. Therefore, even if $k_{-1}$ were 10 times larger than $k_1$, or $k_{-5}$ were 10 times larger than $k_5$, there would be no significant change in the dynamics of the model. A calcium pump has also been incorporated into the plasma membrane. The plasma membrane calcium channels and pumps differ from those of the store membrane by the choice of parameters used in the simulations (Table 1). For both pumps, the Hill coefficient has been set to 2. A fast calcium buffer has been defined for the cytoplasm, serving as a temporary receiver for the large amounts of calcium entering the cell directly after stimulation and simulating both the endogenous buffer and the buffering properties of the fluorescent calcium indicators.

**TABLE 1  Typical values for the parameters used in the simulations**

| Parameter | Definition | Value |
|---|---|---|
| $k_1$ | Rate of calcium release from the store | $7.5 \text{ s}^{-1}$ |
| $k_2$ | Rate of calcium association with the buffer | $601 \ \mu\text{M}^{-1}\text{s}^{-1}$ |
| $k_{-2}$ | Rate of calcium dissociation from the buffer | $97 \text{ s}^{-1}$ |
| $V_3$ | Maximum rate of calcium pumping into the store | $500 \ \mu\text{M/s}$ |
| $K_4$ | Dissociation constant of the store calcium pump | $0.1 \ \mu\text{M}$ |
| $k_5$ | Rate of calcium influx from the external medium | $0.000158 \text{ s}^{-1}$ |
| $V_6$ | Maximum rate of the plasma membrane calcium pump | $1.5 \ \mu\text{M/s}$ |
| $K_7$ | Dissociation constant of the plasma membrane calcium pump | $0.6 \ \mu\text{M}$ |
| $x_{out}$ | Extracellular calcium concentration | $1500 \ \mu\text{M}$ |
| $b_{total}$ | Total concentration of the calcium buffer | $300 \ \mu\text{M}$ |
| $x_{s,i}$ | Initial calcium concentration in the store | $180 \ \mu\text{M}$ |
| $x_{c,i}$ | Initial calcium concentration in the cytoplasm | $0.108 \ \mu\text{M}$ |
| $T_o$ | Basal fractional activity of the channels in the store and plasma membrane | $0.2$ |
| $T$ | Fractional activity of the channels in the store and plasma membrane ($T_o \leq T \leq 1$) | $0.8$ |

We assumed activation of the plasma membrane calcium channel and release of calcium from the stores to be under the control of a cytoplasmic second messenger. To minimize the number of parameters, the concentration of this second messenger has been defined as a linear function of the fractional excitation level of the cell rather than by a receptor binding curve. It is extremely important that the model produce a steady-state solution both before stimulation and after the decay of the initial $[Ca^{2+}]_i$ transient. To achieve this, the partial activation of the channels in the plasma membrane and calcium store has been divided into two terms: a constant term, representing activity at rest ($T_o$); and a variable term, representing activity above $T_o$ after stimulation ($T$). The constant term produces passive calcium leakage from both the store and the extracellular solution into the cytoplasm. Thus a balance between influx and efflux of calcium ions is established, constituting the basis for the steady-state basal $[Ca^{2+}]_i$. The variable term (with a range from $T_o$ to 1) represents the fractional activation of the store and plasma membrane channels induced by membrane receptor mediated activation of the cell. Basal and variable activation values were the same for the calcium channels in both the store and plasma membranes. The above assumptions for the stimulation mechanism in the modeled cell are intended to permit investigation of the dynamics of biphasic calcium transients under the simplest conditions. The components of the model and their interactions are shown schematically in Fig. 1. The kinetic model is described by the following equations:

$$\frac{dx_s}{dt} = -k_1(T + T_o)(x_s - x_c) + V_3 \frac{x_c^2}{K_4^2 + x_c^2} \tag{1}$$

$$\frac{dx_c}{dt} = k_1(T + T_o)(x_s - x_c) - V_3 \frac{x_c^2}{K_4^2 + x_c^2} - k_2 x_c b$$

$$+ k_{-2}(b_{total} - b)$$

$$+ k_5(T + T_o)(x_{out} - x_c) - V_6 \frac{x_c^2}{K_7^2 + x_c^2} \tag{2}$$

$$\frac{db}{dt} = -k_2 x_c b + k_{-2}(b_{total} - b) \tag{3}$$

where $x_c$ is the average cytoplasmic calcium concentration, $x_s$ is the calcium concentration in the intracellular calcium store, and $b$ is the concentration of calcium free buffer in the cytoplasm.

The processes involved in the release of calcium from the store and its active pumping into the store are defined in Eq. 1. The simple scheme of calcium ion binding to the calcium buffer is described by Eq. 3. The dynamics of the calcium concentration in the cytoplasm, described by Eq. 2, includes, in addition to the terms described by Eqs. 1 and 3, the terms describing calcium influx from the external medium and active pumping of this calcium back to the external medium. Constants used in the above equations are

defined in Table 1 together with typical values used in the simulations.

## RESULTS

### Analytical

Elevated calcium plateaus, after the decay of the initial rapid increase in $[Ca^{2+}]_i$, are characteristic of biphasic calcium transients. A crucial test of the integrity of our model is whether it produces such steady-state solutions during stimulation and rest. This steady state should be controlled by the rates of calcium entry and extrusion across the plasma membrane. At steady state, the time derivatives of the model's variables are zero ($dx_s/dt = dx_c/dt = db/dt = 0$). Under these conditions, Eqs. 1–3 produce the following relations:

$$0 = V_3 \frac{x_c^2}{K_4^2 + x_c^2} - k_1(T + T_o)(x_s - x_c) \tag{4}$$

$$0 = k_5(T + T_o)(x_{out} - x_c) - V_6 \frac{x_c^2}{K_7^2 + x_c^2} \tag{5}$$

$$0 = k_{-2}(b_{total} - b) - k_2 x_c b \tag{6}$$

Equation 4 describes the equilibrium between the rates of calcium release from and calcium pumping into the store. Equation 5 describes the equilibrium between the rate of calcium influx from the extracellular medium and the rate of calcium extrusion from the cytoplasm by the plasma membrane calcium pump. Equation 6 describes the balance between the bound and free forms of the cellular calcium buffer. Because the equations are linear for $x_s$ and $b$, for every solution of Eq. 5 there is only one corresponding solution of Eq. 4 and of Eq. 6. Furthermore, because $k_5(T + T_o)(x_{out} - x_c)$ decreases as a function of $x_c$ and $V_6(x_c^2/(K_7^2 + x_c^2))$ increases as a function of $x_c$, Eq. 5 has a unique solution ($x_{c,s}$). Therefore, there exists a unique steady state for the kinetic model defined by Eqs. 1–3 (given by the steady-state values $x_{c,s}$, $x_{s,s}$, $b_s$). Recalling that under physiological conditions $x_{c,s} \ll x_{out}$, it is possible to obtain the following accurate approximation for $x_{c,s}$ from Eq. 5, which can be used to calculate $x_{s,s}$ and $b_s$:

$$x_{c,s} \approx K_7 \sqrt{\frac{k_5(T + T_o)x_{out}}{V_6 - k_5(T + T_o)x_{out}}} \tag{7}$$

$$x_{s,s} = \left(\frac{V_3 x_{c,s}^2}{(K_4^2 + x_{c,s}^2)(T + T_o)k_1} + x_{c,s}\right); \quad b_s = \frac{k_{-2}b_{total}}{k_2 x_{c,s} + k_{-2}} \tag{8}$$

The error in the steady-state values obtained with this approximation, estimated by numerically solving Eq. 5, is less than 0.001%. In Eq. 7 the inequality $V_6 > k_5(T + T_o)x_{out}$ must be maintained for the steady-state value $x_{c,s}$ to be a real number. In other words, to generate a steady state, the maximum rate of pumping must be greater than the rate of calcium influx. The same rationale applies to the calcium

store, where the inequality $V_3 > k_1(T + T_o)x_{s,s}$ must be maintained so $x_{s,s}$ will be a real number. A steady state should also exist before stimulation of the cell ($T = 0$). That steady state represents the balance between the passive leakage and active pumping of calcium across the membranes of both the cell and the calcium store. Because the term $T + T_o$ is linear in Eqs. 4 and 5, the set of equations defining the steady state after stimulation (Eqs. 4–6) also describe the equilibrium state before stimulation. Therefore, there exists a unique set of solutions to Eqs. 1–3 before stimulation, which is the set of initial values of the model's variables ($x_{c,i}$, $x_{s,i}$, $b_i$).

These initial values of the model's variables present an obstacle to the numerical evaluation of the model. The resting value of the intracellular calcium concentration in many types of cells is $\sim 0.1$ $\mu M$, whereas the calcium concentration in the calcium store is on the order of 10–1000 $\mu M$. This large difference among the initial values of the model's variables and the large rate constant of calcium release from the stores (Table 1) cause the rate of calcium release from the intracellular store (appearing in Eqs. 1 and 2) to be considerably faster than the rest of the processes defined in the model. Although the calcium gradient across the cell membrane is greater than the one across the store membrane, the rate of calcium cycling across the cell membrane is much smaller than that across the store membrane (Table 1). Thus it is safe to consider the entry of calcium from the extracellular medium as a slow process. Applying techniques commonly used for the numerical evaluation of ordinary differential equations to this equation set could lead to large computational errors. Therefore we have sought a way to uncouple this fast calcium cycling from the slow one. We accomplished this by introducing the following dimensionless variables:

$$x = \frac{x_c}{x_{c,i}}, \quad y = \frac{x_s + x_c}{x_{s,i} + x_{c,i}} \approx \frac{x_s + x_c}{x_{s,i}}, \quad z = \frac{b}{b_{total}}$$

These variables are of the same order of magnitude. The initial values for the simulations based on Table 1 and Eqs. 7 and 8 would be in the new variables $x = 1$, $y = 1$, $z = 0.6$. Substitution of these variables in Eqs. 1–3 results in the following dynamical system:

$$\gamma \frac{dx}{dt} = \kappa_1(y - 2\gamma x) - \gamma\kappa_3 \frac{x^2}{K_4^2 + \delta^2 x^2} - \gamma\kappa_2 xz$$

$$+ \gamma\kappa_{-2}(1 - z) + \kappa_5(\alpha - \gamma x) - \gamma\kappa_6 \frac{x^2}{K_7^2 + \delta^2 x^2} \tag{9}$$

$$\frac{dy}{dt} = \left(-\gamma\kappa_2 xz + \gamma\kappa_{-2}(1 - z) + \kappa 5(\alpha - \gamma x)\right. \tag{10}$$

$$\left. - \gamma\kappa_6 \frac{x^2}{K_7^2 + \delta^2 x^2}\right)$$

$$\frac{dz}{dt} = -\delta \frac{\kappa_2}{b_{total}} xz + \delta \frac{\kappa_{-2}}{b_{total}} (1 - z) \qquad (11)$$

(The full derivation of this system and the definitions of the new parameters appear in the Appendix.)

In this set of equations, all of the processes occurring at the calcium store appear only in Eq. 9, thus separating the faster variable $x$ from the other variables. The above singularly perturbed system can be investigated in several ways (Aggarwal, 1971). Because the dimension of this equation system is greater than 2, the methods of the quantitative theory of differential equations are generally difficult to apply. Numerical analysis is also of little help when applied to models containing variables that differ by several orders of magnitude. This is exactly as in the case for singularly perturbed systems because of the "stiffness" of the system. In the present work we have used the approach recently suggested by Gold'shtein and Sobolev (1992) for the analysis of such a system based on the theory of integral manifolds (Mitropol'skii and Lykova, 1973; Strygin and Sobolev, 1988). The approximation $\gamma\, dx/dt = 0$ leads to a modification of the quasi-steady-state approximation. The coefficient $\gamma$ is defined as the ratio between the initial values of the calcium concentrations in the cytoplasm and in the calcium store. The smaller $\gamma$ is, the better the approximation $\gamma\, dx/dt = 0$. In our simulations we have used $\gamma = 55 \times 10^{-4}$, which is sufficiently small to provide an accurate approximation. This approximation transformed the system of Eqs. 9–11 from three differential equations into two differential equations (Eqs. 10 and 11) and an algebraic one (Eq. 9) defining a surface in $x$, $y$, $z$ space. In our case this surface is a graph of the function $x = h(y, z)$, thus expressing the fast variable as a function of the slow variables. The slower processes in the model are thus defined as trajectories on this slow surface. When the method of the quasi-steady-state concentrations is used, $x = h(y, z)$ is inserted into the slower equations, which are then analyzed. When the method of integral manifolds is being used to solve a specific problem, a central question is the exact calculation of this manifold. Because an exact calculation is generally impossible, various approximations are necessary. In this paper we use only the zero term of the asymptotic expansion of the manifold in powers of the small parameter $\gamma$. Because Eq. 9 is nonlinear with respect to $x$, the representation $x = h(y, z)$ exists only formally. Therefore, for the explicit calculation, the representation of the slow surface as $y = \Phi(x, z)$ has been used. From this equation it is possible to reobtain $dx/dt$ by using the following relationships:

$$\frac{dy}{dt} = \frac{\partial\Phi}{\partial x}\frac{dx}{dt} + \frac{\partial\Phi}{\partial z}\frac{dz}{dt} \qquad (12)$$

$$\frac{dx}{dt} = \frac{(dy/dt) - (\partial\Phi/\partial z)\,(dz/dt)}{\partial\Phi/\partial x} \qquad (13)$$

Because Eq. 10 is the same $dy/dt$ that appears in Eq. 13, it is possible to reduce the original system of three differential

equations to a new set of only two differential equations:

$$\frac{dx}{dt} = \frac{\begin{array}{l}(-\gamma\kappa_2 xz + \gamma\kappa_{-2}(1 - z) + \kappa 5(\alpha - \gamma x) \\ - \gamma\kappa_6\,(x^2/K_7^2 + \delta^2 x^2)) - (\partial\Phi/\partial z)\,(dz/dt)\end{array}}{\partial\Phi/\partial x} \qquad (14)$$

$$\frac{dz}{dt} = -\delta \frac{\kappa_2}{b_{total}} xz + \delta \frac{\kappa_{-2}}{b_{total}} (1 - z) \qquad (15)$$

## Numerical

In reviewing the literature, we encountered a high degree of variability in the parameters describing the various components of the calcium signaling system. For example, the maximum rate of calcium pumping into the calcium store ranges from 0.9 $\mu$M/s (Keizer and De Young, 1994) to 1038 $\mu$M/s (Tang and Othmer, 1994). A similar problem has been encountered in the parameterization of three other important elements of the model: the rate of calcium release from the stores, the rate of calcium influx, and the maximum rate of calcium extrusion from the cell by the plasma membrane calcium pump. Thus the maximum rate of the store membrane calcium pump has been taken to be in the middle of the range found in the literature. The approximate rate of calcium influx was estimated from the rate of fura-2 quenching by $Mn^{2+}$ influx (Jacob, 1990; Morgan and Jacob, 1994). The rate of fura-2 quenching was evaluated from the average value of $[Ca^{2+}]_i$. Therefore, the value extracted from these measurements is considered to be the best for use in the numerical simulations. The binding constants of the plasma membrane calcium pump and the store membrane calcium pump have been set in the middle of the range found in the literature. It has been shown (Jafri and Keizer, 1995) that the fluorescent dye used for the evaluation of $[Ca^{2+}]_i$ can affect the values obtained because of its binding kinetics to calcium ions. Therefore, the calcium ion association and dissociation constants of the buffer were initially set to be those of fura-2 (Kao and Tsien, 1988). The two remaining parameters of the model, the rate of calcium release from the stores and the maximum rate of calcium pumping by the plasma membrane calcium pump, were estimated from the basal steady state of the model (Eqs. 4 and 5). This estimation requires a knowledge of the values of the model's variables during rest. Whereas the resting cytoplasmic calcium has been measured in many cell types with high reproducibility ($\sim$0.1 $\mu$M), exact information on the concentration of calcium ions in the storage compartment is still lacking. Recently it has been shown that $[Ca^{2+}]_{store}$ is higher than the values previously obtained (Kendall et al., 1992). Therefore we have used the value of 180 $\mu$M as the initial calcium concentration in the storage compartment during rest $(x_{s,i})$ and have decided to keep this value constant in all of the simulations carried out in this work. Using this value, it was possible to obtain the value of $x_{c,i}$ from Eq. 4. The initial concentration of the unbound calcium buffer $(b_i)$ was calculated from Eq. 6.

To test the assumptions made in the analytical treatment of the model, we investigated the behavior of the model directly after the onset of stimulation (Fig. 2). Because Eqs. 14–15 define a trajectory on the slow surface defined by Eq. 9, the numerical integration of these equations should be initiated with values residing on this surface. The result of setting $\gamma \, dx/dt = 0$ in Eq. 9 is a fifth-order polynomial in $x$ that is first order for $y$ and $z$. Knowing the initial calcium concentration in the stores and the concentration of the free calcium buffer before stimulation, it is possible to calculate the initial value of the cytoplasmic calcium concentration on the slow surface by solving Eq. 9 numerically for $x$. For the parameters in Table 1, this gives a $[Ca^{2+}]_i$ initial value on this surface of 0.118 $\mu$M, which is not far from the resting $[Ca^{2+}]_i$ of 0.108 $\mu$M. The results of the simulation carried out with the parameters listed in Table 1 are shown in Figs. 2 and 3. The initial fast change in $[Ca^{2+}]_i$, directly after the stimulation of the system (Fig. 2 A), corresponds to a

decrease in the concentration of the $[Ca^{2+}]_{store}$ (Fig. 2 B) and in $[buffer]_{free}$ (Fig. 2 C). Because the approximation used to derive Eqs. 14–15 is of zero order, these changes carry little information on the kinetics of the model during the first seconds after stimulation. Moreover, because the activation of the cell was modeled as a step from $T_0$ to $T_0 + T$, the changes observed in the variables of the model are by nature faster than the ones observed in the living cell, where the level of $IP_3$ may increase gradually. The changes in the three variables trace a fast trajectory on the slow surface defined by Eq. 9 (Fig. 2 D). This trajectory clearly shows the intimate relationship between the three variables: $[buffer]_{free}$ and $[Ca^{2+}]_{store}$ decrease as $[Ca^{2+}]_i$ increases; $[Ca^{2+}]_{store}$ reaches its minimum when the fluxes of calcium release from and calcium pumping back into the store are equal.

After this initial rapid change, a much slower phase is observed. To view this phase in full, the same simulation is
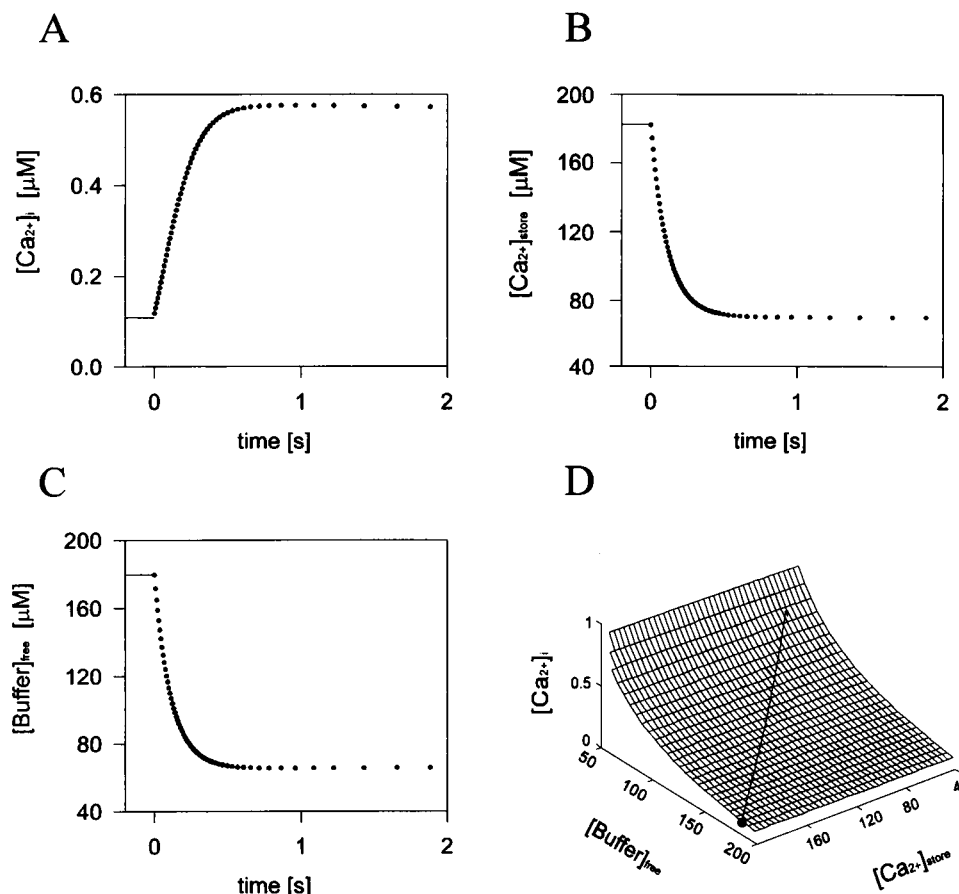


FIGURE 2 Simulation of the initial rapid changes in the variables of the model. The changes in the cytoplasmic calcium concentration (A), the concentration of calcium in the store (B), and the concentration of the free buffer (C) as a function of time are shown. The solid line in these three illustrations marks the values of the variables at rest. The initial values used for the numerical integration were the resting values of $[Ca^{2+}]_{store}$, the resting value of $[buffer]_{free}$, and the value of $[Ca^{2+}]_i$ on the slow surface defined by the algebraic form of Eq. 9. This value was calculated by numerical evaluation of the real roots of the polynomial form of Eq. 9. The three-dimensional surface defined by the algebraic form of Eq. 9 is shown in (D). The values of the variables at rest (●) were plotted on this slow surface and the trajectory traced on following the integration of the model (line). All of the simulations were carried out on an IBM RS-6000-390 computer using custom-made programs in standard C language. Numerical integration was carried out by a fourth-order Runge-Kutta routine with adaptive step control (Press et al., 1992). The roots of Eq. 9 were determined by finding the eigenvalues of the companion matrix of this polynomial (Press et al., 1992). The parameters used for this simulation are from Table 1.
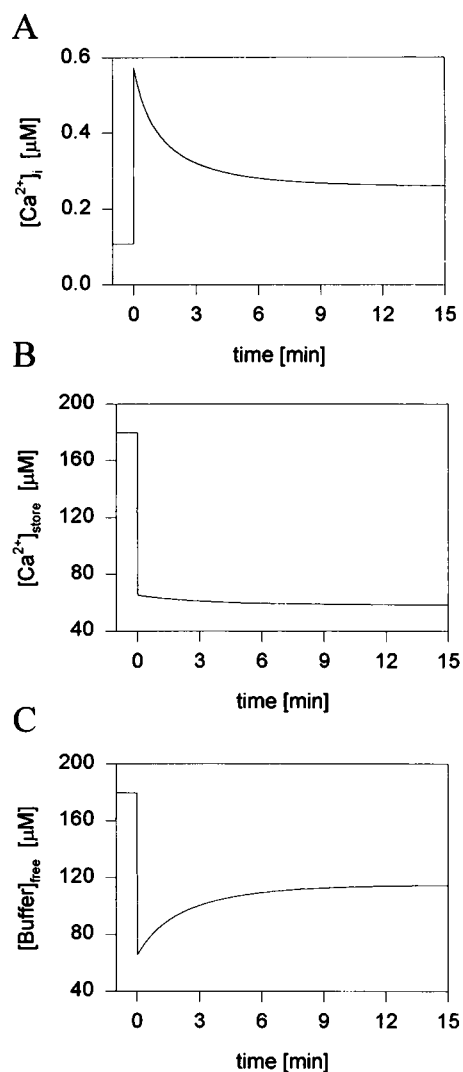
FIGURE 3　A typical biphasic calcium transient produced by numerical integration of the model. The changes in the concentrations of the cytoplasmic calcium (A), store calcium (B), and the calcium free buffer (C) are displayed. The parameters used are from Table 1.

to be a single jump from the initial values to the maximum change in the physiological variables.

The combined effect of discharging the calcium store and opening the calcium channel in the plasma membrane is coordinated by the excitation level of the cell. Increasing the excitation level ($T$) from rest ($T_o$) to the maximum value ($T + T_o = 1$) increases both the maximum rise in $[Ca^{2+}]_i$ and the elevated calcium plateau (Fig. 4 $A$). At the same time, the amount of calcium discharged from the store increases (Fig. 4 $B$) while the $[buffer]_{free}$ decreases (Fig. 4 $C$). Performing the simulation with $T = 0$ results in no changes at all in any of the model's variables (Fig. 4 $A$–$C$, dotted lines). This confirms the prediction made by Eqs. 4–6 that the model has a steady-state solution at rest. We have observed, in rabbit ciliated epithelium, that the value of the elevated calcium plateau and the rate of calcium decay to that plateau increase with the level of cell excitation (Korngreen and Priel, 1996). This pattern has been reproduced by the present model (Fig. 4 $A$). The apparent rate of decay ($k_{app}$) was calculated by fitting an exponential decay to the traces in Fig. 4 $A$. The results are shown in Fig. 4 $D$. As expected from the linear definition of the level of cell excitation in the model, the dependence of the maximum rise in $[Ca^{2+}]_i$, the elevated calcium plateau, and the apparent rate of decay are all linear (Fig. 4 $D$). The dependence of $k_{app}$ on the level of cell excitation is explained by the model in the following manner. Because the plasma membrane calcium pump is of the Hill type, the greater the rise in $[Ca^{2+}]_i$, the faster it will be pumped from the cytoplasm, resulting in a larger $k_{app}$.

It has been suggested (Alkone and Rasmussen, 1988; Rasmussen and Rasmussen, 1990) that after stimulation there is an increase in both the influx of calcium and its extrusion from the cytoplasm by the plasma membrane calcium pump. To examine the behavior of the model under conditions of increased calcium cycling, the values of both $k_5$ and $V_6$ were changed while their ratio was kept constant. This did not change the value of the elevated calcium plateau (Fig. 5 $A$), but did affect the kinetics of the $[Ca^{2+}]_i$ decay from its maximum value. Fast calcium cycling produced fast decays, reaching a steady value in less than 2 min, whereas slow calcium cycling produced slow decays that took more than 15 min of simulation to reach a steady value. The apparent rate of decay was linearly dependent on both $k_5$ and $V_6$ (Fig. 5 $B$).

Because no inactivation of the calcium channel in the calcium store membrane has been incorporated into the model, the store remains partially depleted for the duration of cellular excitation. Once the excitation level is reduced from its maximum value ($T = 0.8$) to the resting level ($T = 0$), the $[Ca^{2+}]_i$ decreases from the elevated plateau to a value slightly lower than its value at the beginning of the simulation (Fig. 6 $A$), followed by a slow increase in $[Ca^{2+}]_i$ to its initial value. The amount of calcium in the store increased almost to its initial value (Fig. 6 $B$), and the concentration of the free calcium buffer increased to a value above its initial value (Fig. 6 $C$). It is clear from this

shown in Fig. 3 over a much longer time scale. The simulated curve in Fig. 3 $A$ is characteristic of biphasic calcium transients, similar to results we have observed experimentally (Korngreen and Priel, 1996). The $[Ca^{2+}]_i$ decays, over several minutes, from the maximum value reached in the initial rapid phase to a stable value greater than the resting $[Ca^{2+}]_i$, whereas $[Ca^{2+}]_{store}$ (Fig. 3 $B$) and $[buffer]_{free}$ (Fig. 3 $C$) level off on the same time scale. These slow changes trace a trajectory on the slow surface defined by Eq. 9 (not shown). Inserting the model's parameters into Eqs. 4–6, it is possible to calculate the steady-state solution for the simulation in Fig. 3. The values obtained agree with the results of the numerical simulation. Because we are interested in the characteristics of biphasic calcium transients, all of the simulations have been carried out on a time scale of minutes. Within this time scale, the initial rapid rise appears
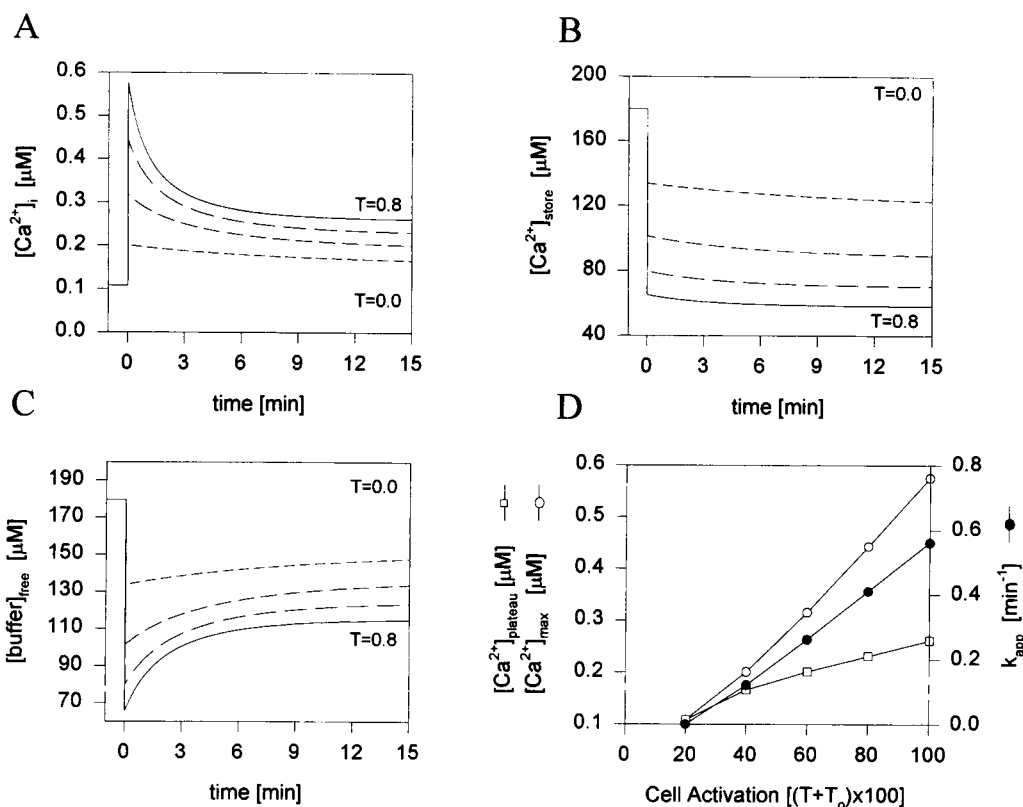
FIGURE 4 The dependence of the biphasic calcium transients on the level of cell excitation. Reducing the level of cell excitation (T) decreases the height of the initial [Ca$^{2+}$]$_i$ spike (A), lowers the elevated calcium plateau (A), decreases the amount of calcium discharged from the store (B), and increases the amount of free calcium buffer (C). The values of T used in the simulations were 0.8 (solid line), 0.6 (long dashes), 0.4 (medium dashes), 0.2 (short dashes), and zero (dotted line). The maximum and minimum values of T (0.8 and 0.0) are shown near the first and last lines in each panel to help in the identification of each simulation. The increase in [Ca$^{2+}$]$_i$ spike height (O), the increase in calcium plateau (□), and the apparent rate of calcium decay (●) were all dependent on the level of cell excitation (D).

simulation that the calcium store is refilled primarily by calcium released from the fast buffer, with only a small amount coming from the extracellular medium. When Eq. 9 was transformed into an algebraic form, the parameters determining the form of the simulated calcium transient were fixed for the duration of the simulation, defining a specific slow surface. To change the excitation level of the cell, it was necessary to recalculate the change in [Ca$^{2+}$]$_i$ from the polynomial form of Eq. 9 and restart the simulation. As initial conditions for this calculation, the values of y and z at the elevated steady state were taken.

When calcium concentration in the extracellular solution was lowered to 0.1 μM, the initial rise in [Ca$^{2+}$]$_i$ was not affected, but the elevated calcium plateau was abolished (Korngreen and Priel, 1996). Performing the simulation at an extracellular calcium concentration of 0.1 μM ($x_{out}$ = 0.1) results in the elimination of the elevated calcium plateau (Fig. 7 A). After the rapid decay of the initial transient, the [Ca$^{2+}$]$_i$ (Fig. 7 A) and the [Ca$^{2+}$]$_{store}$ (Fig. 7 B) continue to decay slowly. When the simulation is run for 30 min, it is observed that this decay continues until most of the calcium remaining in the store is depleted (data not shown). In experiments carried out on ciliary epithelium (Korngreen

and Priel, 1996), we have shown that increasing the calcium concentration back to the physiological level of 1500 μM results in an increase in [Ca$^{2+}$]$_i$ to the same elevated plateau observed under normal conditions. Increasing external calcium to 1500 μM after 15 min of the simulation gives essentially the same result as obtained experimentally. As seen in Fig. 7 A, there is a slow increase in [Ca$^{2+}$]$_i$ that levels off to the same elevated plateau value observed in the simulation performed at normal extracellular calcium concentration (cf. Fig. 6 A). In addition, both the [Ca$^{2+}$]$_{store}$ (Fig. 7 B) and the [buffer]$_{free}$ (Fig. 7 C) slowly approach steady-state values identical to those calculated from Eqs. 4–6. The $k_{app}$ calculated for the calcium decay in Fig. 6 A ($x_{out}$ = 1500 μM) was 0.658 min$^{-1}$, whereas the $k_{app}$ calculated from the decay in Fig. 7 A ($x_{out}$ = 0.1 μM) was 1.09 min$^{-1}$. This 1.65-fold increase is in good agreement with the experimental result of a 2.4-fold increase (Korngreen and Priel, 1996).

A widely used tool for the investigation of calcium transients is the pharmacological agent thapsigargin, a highly potent and specific inhibitor of the calcium store pump commonly found in the endoplasmic reticulum. After the inhibition of this pump, the calcium passively leaks out of
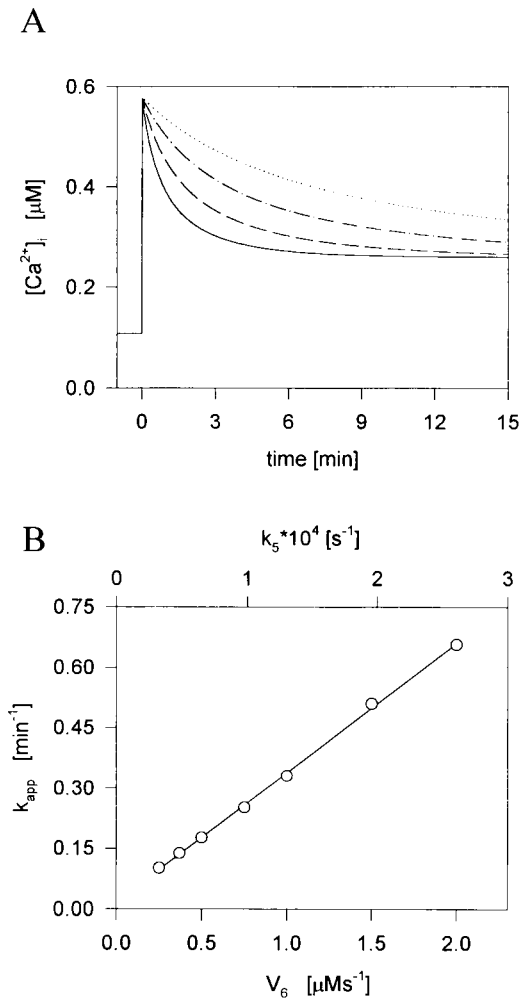
## A



## B



FIGURE 5 The effect of increased calcium cycling across the plasma membrane on simulated biphasic calcium transients. The ratio between the rate of calcium influx and calcium pumping across the plasma membrane determines the level of the elevated calcium plateau. Keeping this ratio constant while changing the values of $k_5$ and $V_6$ by the same factor did not affect the value of the elevated plateau, but did have a marked effect on the kinetics of the $[Ca^{2+}]_i$ decay (A). The $k_5$-$V_6$ pairs used in the simulations shown in A were $2.63 \times 10^{-5}$ $s^{-1}$ and 0.25 $\mu M/s$ (dotted line), $5.26 \times 10^{-5}$ $s^{-1}$ and 0.5 $\mu M/s$ (dash-dot line), $1.05 \times 10^{-4}$ $s^{-1}$ and 1 $\mu M/s$ (dashed line), and $2.65 \times 10^{-4}$ $s^{-1}$ and 2 $\mu M/s$ (solid line). The two upper traces in A do not appear to decay to the elevated plateau within the 15-min time scale. However, when the simulation was carried out for 30 min, both traces decayed to the same elevated calcium plateau as the lower traces (not shown). The apparent rate of calcium decay ($k_{app}$) was evaluated by calculating the slope of the natural logarithm of the calcium decay after subtraction of the elevated plateau. The apparent rate of decay is shown as a function of $V_6$ and $k_5$ (B). All of the parameters used in the simulations shown in this figure, except for $k_5$ and $V_6$, are from Table 1.

the store until the store eventually empties. This enables the direct activation of calcium-dependent cellular processes without activation of the cell by the membrane receptor. Experiments with thapsigargin are routinely carried out with extracellular solutions that do not contain calcium, a procedure established after it was found that store depletion with thapsigargin could activate a calcium influx (Takemura et al., 1989). Activation of the cell by a membrane receptor
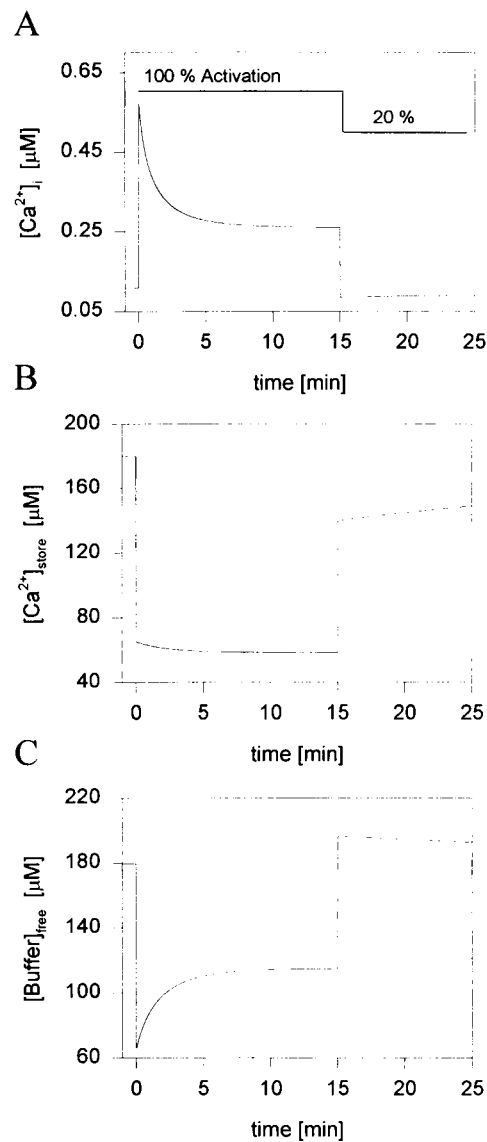
## A



## B



## C



FIGURE 6 Rapid refill of the calcium stores after reduction in the level of cell stimulation. Fifteen minutes after the beginning of the simulation, the value of $T$ was lowered from 0.8 to 0, leaving the model at a resting activity of 20%. The resulting changes in $[Ca^{2+}]_i$ (A), the calcium concentration in the store (B), and the free calcium buffer (C) are shown.

after such calcium store depletion usually does not result in a noticeable rise in $[Ca^{2+}]_i$. To simulate the depletion of the stores by thapsigargin, the value of the maximum rate of calcium pumping into the stores ($V_3$) was lowered by 95%, and the extracellular calcium concentration was lowered to 0.1 $\mu M$. Because the cell is not being activated by the receptor, the activity of the calcium channels of the calcium store and of the plasma membrane were also set at the basal activity of 20% ($T = 0$). The rise in $[Ca^{2+}]_i$ induced by this simulated store depletion was greater than that commonly seen with thapsigargin (Fig. 8 A). The action of thapsigargin is longer than the activation of the cell by the membrane receptor, because of the slow accumulation of the drug in the cell, producing relatively slow rises in $[Ca^{2+}]_i$. This is a
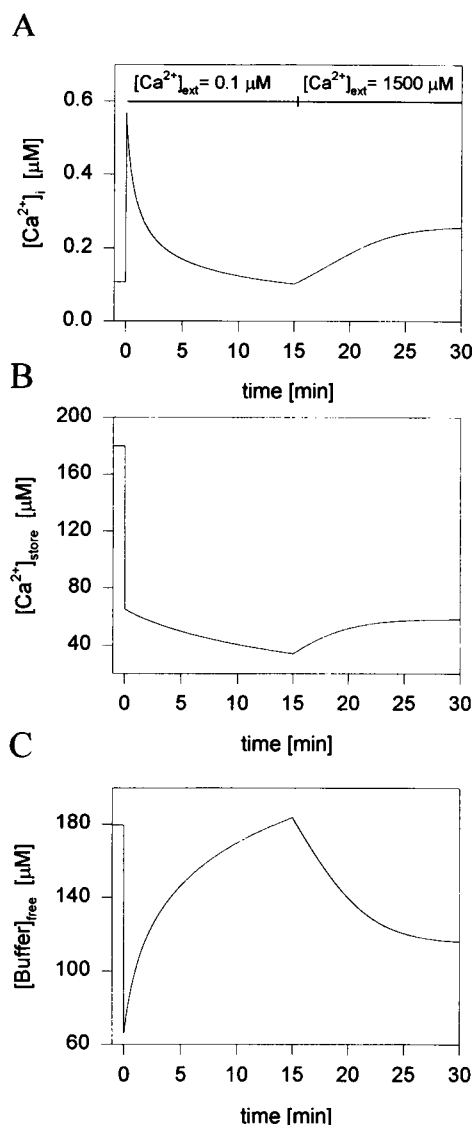
A



B



C



FIGURE 7  Effect of lowering the extracellular calcium concentration on the release and refill of calcium. The simulation was carried out with the parameters listed in Table 1, except for $V_6 = 2$ and $x_{out} = 0.1$. The $[Ca^{2+}]_i$ decayed back to its initial value (A). Fifteen minutes after the beginning of the simulation, the value of $x_{out}$ was increased from 0.1 to 1500 $\mu$M, resulting in an increase in $[Ca^{2+}]_i$ to an elevated plateau. The changes in $[Ca^{2+}]_i$ (A), the calcium concentration in the store (B), and the unbound calcium buffer (C) are displayed.

likely cause for the difference between simulated and experimental traces. After the $[Ca^{2+}]_i$ had decayed to its initial value (15 min from the beginning of the simulation), the activation level of the cell was increased to 100% ($T = 0.8$), simulating the activation of the cell by agonist binding to the membrane receptor. This resulted in a small increase in $[Ca^{2+}]_i$ due to the release of the residual calcium left in the store (the residual calcium concentration was 9 $\mu$M). Performing the same simulation with the normal concentration of extracellular calcium ($x_{out} = 1500$ $\mu$M) produced the graph shown in Fig. 8 B. Thus after store depletion, increasing the level of cell excitation to 100% resulted in a small

jump in $[Ca^{2+}]_i$ due to release of residual calcium from the store and a slow increase in $[Ca^{2+}]_i$ to the elevated plateau induced by calcium influx.

A third scenario, termed capacitative calcium entry (CCE), involves the activation of calcium influx through depletion of the calcium stores rather than by the membrane receptor. Thus the excitation level of the calcium channel in the plasma membrane was set at maximum ($T = 0.8$) from the beginning of the simulation. The simulation, shown in Fig. 8 C, was carried out at normal extracellular calcium concentration. Therefore, after the discharge of calcium from the store, $[Ca^{2+}]_i$ decayed to an elevated plateau. Further stimulation of the modeled cell by the membrane receptor (accomplished by increasing the activation of the store calcium channel from 20% to 100%) resulted in discharge of the residual amount of calcium from the store.

It is possible that depletion of the stores will activate a calcium influx via a nonreceptor-activated pathway. To examine this possibility, we performed the same simulation as described in Fig. 8 C, except that when the cell was stimulated by the agonist (15 min after the beginning of the simulation), the excitation level of the plasma membrane calcium channels was further increased from $T = 0.8$ to $T = 1.6$. This simulated the opening of the receptor-operated calcium channel in the plasma membrane in addition to the capacitative entry of calcium activated by thapsigargin at the beginning of the simulation. As expected, the calcium concentration did not decay to the level before receptor stimulation as in Fig. 8 C, but rather increased to a more elevated plateau (Fig. 8 D). The four simulated experiments shown in Fig. 8 suggest a possible experimental protocol for distinguishing between receptor-activated calcium influxes and store depletion-activated calcium influxes. With small modifications, our model has been able to simulate complete experiments carried out in many previous investigations of the dynamics of intracellular calcium.

The final aspect of calcium transients we have investigated with our model is the role of cytoplasmic calcium buffering. It is clear from the definition of the steady state of the model (Eqs. 4–6) that any changes in buffering capacity should not influence the steady-state solution. However, it seems reasonable to assume that changing the rate of calcium ion association with or dissociation from the buffer might alter the kinetics of the calcium transients in the cytoplasm. To examine this, the calcium buffer binding constants initially set at the values for fura-2 were changed to those for indo-1 and rhod-2. The rates of association for these materials were assumed to be similar ($k_2 = 601$ $\mu M^{-1}$ $s^{-1}$). The rates of dissociation ($k_{-2}$) were calculated from the equilibrium constants of these fluorescent calcium dyes (230 nM for indo-1 and 570 nM for rhod-2). As predicted by the steady-state equations, changing the properties of the buffer changed neither the value of the elevated calcium plateau (Fig. 9 A) nor the steady-state value of the $[Ca^{2+}]_{store}$ (Fig. 9 B). However, changing $k_{-2}$ changed both the maximum rise in $[Ca^{2+}]_i$ and the decay kinetics (Fig. 9 A). It is interesting to note that changing $k_{-2}$ from that of
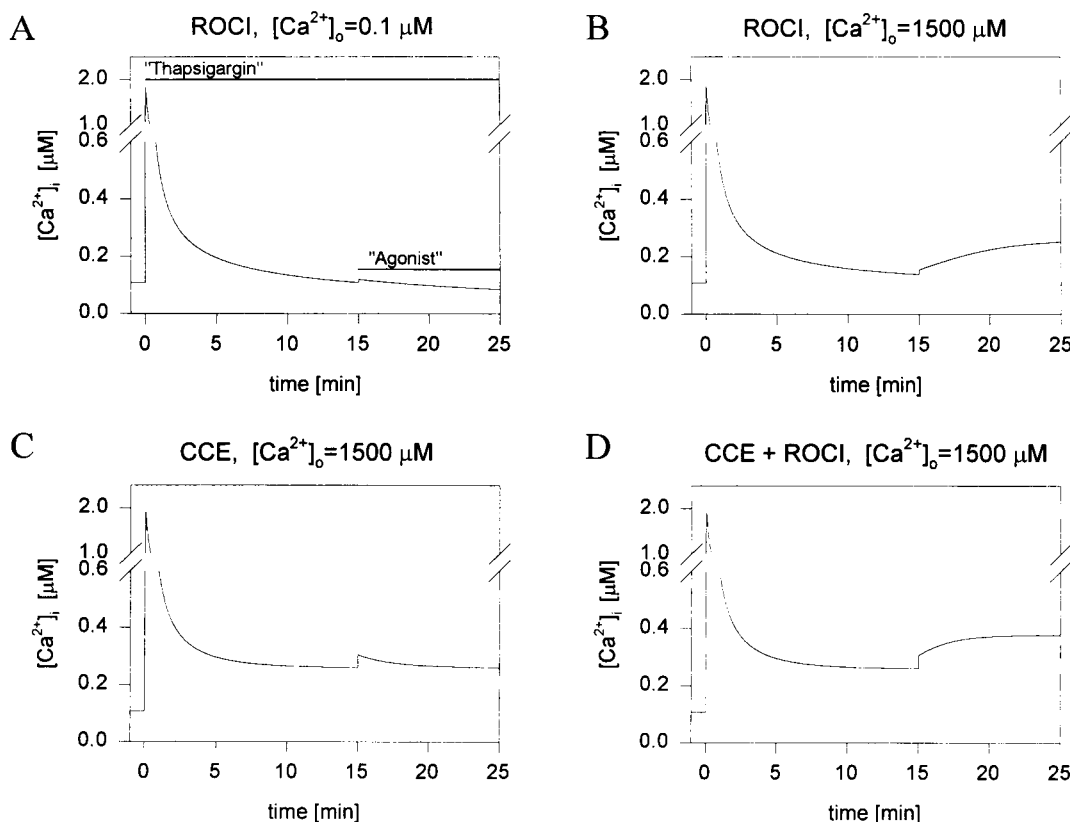
FIGURE 8 Simulated calcium store depletion experiments with thapsigargin. To best mimic the conditions during store depletion with thapsigargin, the level of cell excitation was held at rest ($T = 0$) while $V_3$ was lowered by 95% (from 500 to 25 $\mu Ms^{-1}$) to simulate the inhibition of the calcium store pump. (A) After the initial increase in $[Ca^{2+}]_i$ induced by the store depletion decayed back to its initial value, $T$ was increased to 0.8 (15 min after initiation of the simulation), simulating the activation of the cell by agonist binding to the receptor, followed by receptor operated calcium influx (ROCI). This simulation was carried out with $x_{out} = 0.1$ $\mu M$, as indicated in the title of this panel. To simulate normal extracellular calcium concentrations, the same simulation was run with $x_{out} = 1500$ $\mu M$ (B). To simulate store depletion-activated capacitative calcium entry (CCE), the value of $T$ was set at 0.8 for the plasma membrane calcium channel from the beginning of the simulation and at 0.0 for the store calcium channel. After the elevated plateau was reached (15 min), $T$ for the store calcium channel was also increased to 0.8 (C). When the depletion of the store activates capacitative calcium entry and the agonist activates a receptor-activated calcium influx independently, the net influx of calcium from both open channels is greater than for each of them separately. Therefore, the level of cell excitation was increased from $T = 0.8$ to $T = 1.6$ in D after the stimulation of the cell with agonist.

fura-2 (97 s$^{-1}$) to that of indo-1 (138 s$^{-1}$) elicited a small change in the kinetics of $[Ca^{2+}]_i$ decay and a small decrease in the maximum rise in $[Ca^{2+}]_i$, whereas increasing $k_{-2}$ further to that of rhod-2 (342 s$^{-1}$) resulted in an increase in the maximum rise in $[Ca^{2+}]_i$ (Fig. 9 A). When $k_{-2}$ was varied from 60 s$^{-1}$ to 400 s$^{-1}$, the rise in $[Ca^{2+}]_i$ reached a minimum at $k_{-2} = 140$ s$^{-1}$ (not shown). The probable explanation for this minimum is simply that buffering systems are at maximum capacity when the bound and unbound buffer species are present in equal concentrations. When $k_{-2}$ is slower than 140 s$^{-1}$, the majority of the buffer is in the calcium-bound form, with little in the unbound form. When $k_{-2}$ is faster than 140 s$^{-1}$, the majority of the buffer is in the unbound form, with little in the bound form. In both cases, the result is a higher rise in $[Ca^{2+}]_i$. The decrease in the buffer capacity as $k_{-2}$ increases is clearly seen in Fig. 9 C, which shows the changes in the $[buffer]_{free}$ concentration. Because the initial values of $[buffer]_{free}$ differ from buffer to buffer, the $[buffer]_{free}$ has been normalized to

its initial value, so that relative changes will be more clearly visible. When both binding constants were changed without changing the equilibrium constant, no effect on either the magnitude or the kinetics of the calcium transients was observed (not shown).

## DISCUSSION

The present study shows that a kinetic model using realistic parameters and assumptions produces biphasic calcium transients similar to those observed experimentally (Korngreen and Priel, 1993, 1994, 1996). The properties of the simulated calcium transients were sensitive to the values of the parameters of the model. The model predicted that the maximum rise in $[Ca^{2+}]_i$, the elevated calcium plateau, and the apparent rate of calcium decay were dependent on the level of cell excitation (Fig. 4). The rate of calcium decay was shown to relate to the rate of calcium cycling across the
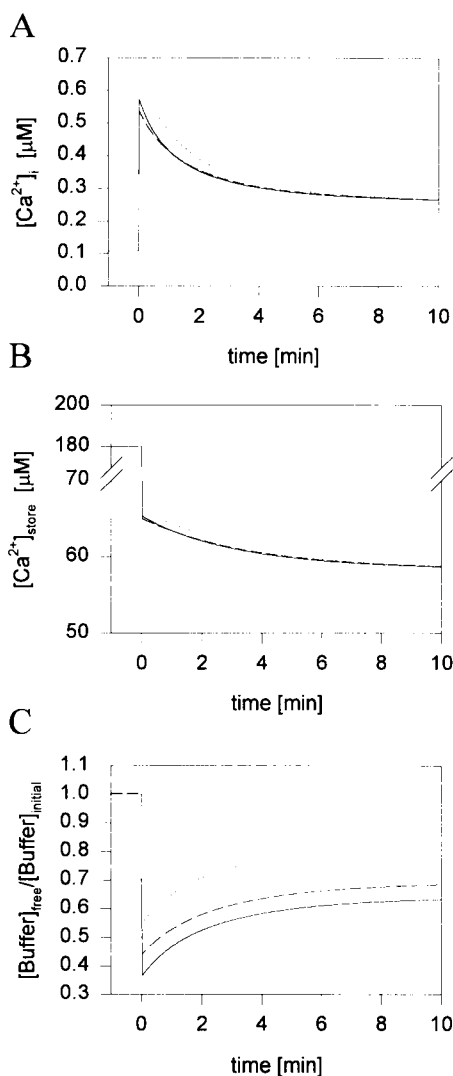
FIGURE 9   Effect of different calcium buffers on the dynamics of the model: changes in $[Ca^{2+}]_i$ (A), $[Ca^{2+}]_{store}$ (B), and $[buffer]_{free}$ (C) for the $k_{-2}$ of fura-2 (97 $s^{-1}$, solid lines), indo-1 (138 $s^{-1}$, dashed lines), and rhod-2 (342 $s^{-1}$, dotted lines).

plasma membrane (Fig. 5). Experiments involving the washout of an agonist from the solution bathing the cell (Fig. 6), elimination of the elevated calcium plateau by lowering of the extracellular calcium concentration (Fig. 7), and calcium store depletion with thapsigargin (Fig. 8) were simulated. Finally, the effect on temporal changes in $[Ca^{2+}]_i$ of several fluorescent dyes, acting as calcium buffers, was examined (Fig. 9).

Accurate numerical integration of the model was made possible by application of the analytical method proposed by Gold'shtein and Sobolev (1992). This permitted the computation of realistic biphasic calcium transients under initial conditions ranging over more than four orders of magnitude and uncoupled the fast calcium cycling of the calcium store from the slower cycling of the plasma membrane. Without such a separation, whether by physical or mathematical means, it would be very hard to produce

accurate simulations. In the calculation of the initial $[Ca^{2+}]_i$ on the slow surface defined by Eq. 9, the computations showed that for the parameters listed in Table 1 and for a resting value of $[Ca^{2+}]_i$ of 0.108 $\mu M$, the initial $[Ca^{2+}]_i$ on the slow surface was 0.118 $\mu M$, thus demonstrating that the dynamic system at rest is not far from the reaction surface that defines the behavior of the system during excitation. Therefore, the system can be activated easily and without the investment of much energy by the cell.

Another approach to solving the problem is to use calcium diffusion through the cell, which has been employed successfully to simulate the progression of calcium waves (Dupont and Goldbeter, 1994; Sneyd et al., 1995; Jafri, 1995). We have preferred at this stage not to add the spatial dimension to the model, to keep it as simple as possible. After the uncoupling of the fast processes from the slow ones, several key features of the model became apparent. The most prominent one was that the calcium stores did not completely deplete (Figs. 3 and 4), but remained as much as one-third full, even at $k_1$ values that produced calcium transients similar in magnitude to those observed experimentally (Figs. 2 and 3). This is due to the high rate of calcium cycling across the calcium store membrane. In vivo, this is achieved by the spatial localization of the discharge of calcium from the store. The high calcium concentration adjacent to the store creates a local "hot spot" of calcium that diffuses into the cytoplasm and induces the calcium pump in the store's membrane to pump calcium back into the store at a high rate. An additional prediction of the model, closely related to the previous one, is that a large portion of the calcium released from the store is maintained in the cytoplasm bound to the cytoplasmic buffer. This was readily observed in Fig. 6, where, upon removal of the agonist, the initial refill of the stores was supplied by calcium released from the calcium buffer. Only a relatively small part of the store remained to be refilled by the calcium influx from the extracellular medium. This prediction of the model is more likely, in our opinion, than the suggestion that most of the calcium released from the store is removed entirely from the cell (Wiesner et al., 1996), which would require a much larger investment of cellular energy.

Another problem resolved by the computational separation of fast events from slow events is the issue of the influence on $[Ca^{2+}]_i$ of the pumping rate of calcium into the store. Because the model has no spatial dimensions, the pump in the store and the pump in the plasma membrane act on the same number of calcium ions. Therefore, when the system in its original form (Eq. 1–3) was integrated, the pump in the store membrane overpowered the weaker pump in the plasma membrane, creating very fast and uncharacteristic decays in $[Ca^{2+}]_i$ (simulations not shown). In vivo, after the discharge of calcium from the store and the return to near-equilibrium, the store becomes kinetically "invisible" because of the balanced rates of release and resequestration. We believe that in the area juxtaposed to the store, a membrane-localized, higher calcium concentration is es-

tablished, which does not extend far enough into the cell to be detected.

These observations on calcium dynamics across the calcium store membrane were used to examine some common experimental protocols. In almost every study on the dynamics of calcium signaling by an agonist binding to a membrane receptor, the response of the system is determined as a function of the concentration of that agonist. Such a dose-response curve was simulated in Fig. 4. From this simulation it was possible to predict that the maximum rise in $[Ca^{2+}]_i$ would be dependent on the level of cell excitation. Furthermore, the level of the elevated calcium plateau and the apparent rate of calcium decay were also shown to be dependent on the level of excitation (Fig. 4 D). This may prove beneficial in the analysis of experimental biphasic calcium transients. If all three experimental parameters are found to be dependent on agonist concentration, as, for example, in our research on ciliated airway epithelium (Korngreen and Priel, 1996), this may serve to strengthen the case for the dual activation of calcium influx and calcium release. The model presented in this work incorporated, for the sake of simplicity, a linear term describing the level of cell excitation $(T + T_o)$. Hence the dependences of both the maximum rise in $[Ca^{2+}]_i$ and the elevated calcium plateau were linear (Fig. 4 D). A relatively simple extension of the model would be the conversion of this linear term to one describing the binding curve of the agonist to the receptor and the kinetics of $IP_3$ synthesis. There are experimental conditions where the elevated calcium plateau is not dependent on the concentration of the agonist, as, for example, when calcium influx is activated by the depletion of the calcium store rather than by agonist binding to the receptor. Such calcium influx, induced by depletion of the calcium store, can be achieved by pharmacological agents such as thapsigargin. The simulations shown in Fig. 8 suggest a possible experimental protocol for differentiating between calcium influxes activated by a receptor (Fig. 8 B), by the calcium store depletion (Fig. 8 C), or by both (Fig. 8 D).

Another common experimental procedure used to probe refilling kinetics of calcium stores is the "double-exposure" technique. In such experiments, the calcium store is discharged by an agonist that is subsequently washed out of the solution. Then, at increasing time intervals, the store is redischarged and the magnitude of the rise in $[Ca^{2+}]_i$ is compared to that of the first discharge. The rationale is that after the first exposure, which causes the store to discharge all or part of its calcium content, the store refills. The second exposure to the agonist then determines the relative content of the store at a given time during this refill process. Our simulations have shown (Fig. 6) that after the washout of the agonist, the initial refill of the stores is fast, on the same time scale as the release, and that it is primarily due to the calcium released from the buffer. After this fast change, $[Ca^{2+}]_{store}$ increases slowly toward its initial value, as seen in Fig. 6 B. This slow increase is due to the contribution of calcium leakage from the external medium rather than to the

activity of the calcium pump in the store membrane. Therefore, the second discharge in the "double-exposure" protocol should not be interpreted directly as the residual content of the stores. Thus the experimental procedure of "double exposure" may not present a complete picture of the kinetics of calcium resequestration into the store.

The calcium signaling system is far more complex than the model presented in this work. Several pharmacologically distinct calcium stores have been identified within the same cell type (Tribe et al., 1995; Korngreen and Priel, 1996). Local increases in the calcium concentration have been observed (Bootman and Berridge, 1995). It has been shown that the cytoplasm contains both mobile and immobile calcium buffers (Zhou and Neher, 1993). Calcium imaging has established the existence of intracellular (Lechleiter et al., 1991) and intercellular (Boitano et al., 1992) calcium waves. In many cell types, oscillations in $[Ca^{2+}]_i$ have been observed (Tsien and Tsien, 1990). These oscillations have been described extensively by many theoretical models over the last decade (Cuthberson and Chay, 1991; Eichwald and Keizer, 1993; Friel, 1995; Kraus and Wolf, 1992; Mayer and Stryer, 1988; Tang and Othmer, 1995). Unfortunately, the large variability between the calcium signaling systems of different cells has proved a great obstacle to describing with a single model the dynamics of even nonoscillating calcium homeostasis. This variability can be seen in the different models suggested for various systems. Recently a model describing the dynamics of non-oscillating calcium transients in human umbilical vein endothelial cells was presented (Wiesner et al., 1996). Several features of this detailed model made comparison to our proposed model difficult. The activation of the endothelial cell was described by the irreversible activation of the thrombin receptor, whereas in our model it was controlled by the reversible activation of a linear receptor. The thrombin receptor directly activated only the calcium store, whereas in our model the receptor activated both the release from the store and the increase in the influx of calcium. As a result, the elevated calcium plateau, a major element of our proposed model, was not sensitive to the concentration of thrombin in the model proposed for endothelial cells. Because the rate of calcium influx was similar to the rate of calcium release from the store in the endothelial cell model, an increase in this rate resulted not only in a higher elevated calcium plateau, but also in a considerable increase in the magnitude of the maximum rise in $[Ca^{2+}]_i$. We have shown experimentally that the maximum rise in $[Ca^{2+}]_i$ in airway ciliated epithelium is not affected by calcium influx, but is due rather only to the release of calcium from stores. Based on this observation, we selected a different set of parameters (detailed in the results), which necessitated analytical treatment of the model before numerical simulation could be carried out. As more accurate data become available on the parameters of the various components of the calcium signaling system, it should become possible to compare different cell types more easily, which, it is hoped, will provide a more unifying model for this essential signaling system.

The model proposed here was intended to provide a solid foundation on which to progress toward this more accurate model. Because our model is based on relatively simple mathematics, it is possible to use analytical tools to determine its validity. Having laid this cornerstone, it is now possible to establish a working dialogue between experiment and theory to revise the model and expand it. Only such a dialogue will make possible the accurate expansion of the model and verification of each addition.

The model presented in this work was able to reproduce several key features of biphasic calcium transients observed experimentally in rabbit ciliated airway epithelium (Korngreen and Priel, 1996). The main feature reproduced was the decay of the calcium concentration in the cytoplasm to a steady plateau higher than its initial value after the initial rise of calcium from the intracellular calcium store. The dependence of the maximum rise in $[Ca^{2+}]_i$, the value of the elevated calcium plateau, and the apparent rate of calcium decay on the level of cell excitation (Korngreen and Priel, 1996) were also reproduced. Several simulated experiments that might help identify the coactivation of calcium release and calcium influx (similar to that observed by us in ciliated cells) have been suggested. These experiments included the depletion of the calcium store with pharmacological agents and the effect of the concentration of the extracellular calcium on the elevated calcium plateau. It is therefore our belief that the model will be helpful to experimentalists facing the problem of identifying and characterizing this pattern of cellular activation.

## APPENDIX

Transforming Eqs. 1–3 with the new variables,

$$x = \frac{x_c}{x_{c,i}}, \quad y = \frac{x_s + x_c}{x_{s,i} + x_{c,i}} \approx \frac{x_s + x_c}{x_{s,i}}, \quad z = \frac{b}{b_{total}}$$

results in the following system:

$$x_{c,i}\frac{dx}{dt} = k_1(T + T_o)(x_{s,i}y - 2x_{c,i}x) - V_3\frac{x_{c,i}^2 x^2}{K_4^2 + x_{c,i}^2 x^2}$$

$$- k_2 x_{c,i} b_{total} xz + k_{-2} b_{total}(1 - z) \qquad (A1)$$

$$+ k_5(T + T_o)(x_{out} - x_{c,i}x) - V_6\frac{x_{c,i}^2 x^2}{K_7^2 + x_{c,i}^2 x^2}$$

$$(x_{c,i} + x_{s,i})\frac{dy}{dt} = - k_2 x_{c,i} b_{total} xz + k_{-2} b_{total}(1 - z)$$

$$+ k_5(T + T_o)(x_{out} - x_{c,i}x) - V_6\frac{x_{c,i}^2 x^2}{K_7^2 + x_{c,i}^2 x^2} \qquad (A2)$$

$$b_{total}\frac{dz}{dt} = - k_2 x_{c,i} b_{total} xz + k_{-2} b_{total}(1 - z) \qquad (A3)$$

Eq. A1 is divided by $x_{s,i}$ and rearranged to produce the form

$$\left(\frac{x_{c,i}}{x_{s,i}}\right)\frac{dx}{dt} = k_1(T + T_o)\left(y - 2\left(\frac{x_{c,i}}{x_{s,i}}\right)x\right)$$

$$- V_3 x_{c,i}\left(\frac{x_{c,i}}{x_{s,i}}\right)\frac{x^2}{K_4^2 + x_{c,i}^2 x^2} - k_2\left(\frac{x_{c,i}}{x_{s,i}}\right)b_{total}xz$$

$$+ \frac{k_{-2} b_{total}}{x_{c,i}}\left(\frac{x_{c,i}}{x_{s,i}}\right)(1 - z) + k_5(T + T_o)$$

$$\times \left(\frac{x_{out}}{x_{s,i}} - \left(\frac{x_{c,i}}{x_{s,i}}\right)x\right) - V_6 x_{c,i}\left(\frac{x_{c,i}}{x_{s,i}}\right)\frac{x^2}{K_7^2 + x_{c,i}^2 x^2}$$

From this equation the following new parameters are defined:

$$\gamma = \left(\frac{x_{c,i}}{x_{s,i}}\right), \quad \delta = x_{c,i}, \quad \kappa_1 = k_1(T + T_o),$$

$$\kappa_{-2} = \frac{k_{-2} b_{total}}{x_{c,i}}, \quad \kappa_2 = k_2 b_{total}, \quad \kappa_3 = V_3 x_{c,i}$$

$$\kappa_5 = k_5(T + T_o), \quad \kappa_6 = V_6 x_{c,i}, \quad \alpha = \frac{x_{out}}{x_{s,i}}$$

Insertion of these new parameters into Eq. A4 results in Eq. 9. Similarly, Eq. A2 is divided by $(x_{c,i} + x_{s,i})$:

$$\frac{dy}{dt} = - k_2 b_{total}\left(\frac{x_{c,i}}{(x_{c,i} + x_{s,i})}\right)xz + \frac{k_{-2} b_{total}}{x_{c,i}}\left(\frac{x_{c,i}}{(x_{c,i} + x_{s,i})}\right)$$

$$\cdot (1 - z) + k_5(T + T_o)\left(\left(\frac{x_{out}}{(x_{c,i} + x_{s,i})}\right) - \left(\frac{x_{c,i}}{(x_{c,i} + x_{s,i})}\right)x\right)$$

$$- V_6 x_{c,i}\left(\frac{x_{c,i}}{(x_{c,i} + x_{s,i})}\right)\frac{x^2}{K_7^2 + x_{c,i}^2 x^2} \qquad (A5)$$

Using the new parameters, it is possible to write

$$\left(\frac{x_{c,i}}{(x_{c,i} + x_{s,i})}\right) = \frac{\gamma}{\gamma + 1} \approx \gamma$$

and

$$\left(\frac{x_{out}}{(x_{c,i} + x_{s,i})}\right) = \frac{\alpha}{\gamma + 1} \approx \alpha$$

Using this transformation with the rest of the new parameters Eq. A5 gives Eq. 10. Using only the new parameters, Eq. A3 gives Eq. 11.

## REFERENCES

Aggrawal, J. K. 1971. Notes on Nonlinear Systems. Van Nostrand, New York.

Alfahel, E., A. Korngreen, A. H. Parola, and Z. Priel. 1996. Purinergically induced membrane fluidization in ciliary cells: characterization and control by calcium and membrane potential. Biophys. J. 70:1045–1053.

Alkone, D. L., and H. Rasmussen. 1988. A spatial-temporal model of cell activation. Science. 239:998–1005.

Benham, C. D., and R. W. Tsien. 1987. A novel receptor-operated $Ca^{2+}$-permeable channel activated by ATP in smooth muscle. *Nature.* 328: 275–278.

Berlin, J. R., J. W. M. Bassani, and D. M. Bers. 1994. Intrinsic cytosolic calcium buffering properties of single rat cardiac myocytes. *Biophys. J.* 67:1775–1787.

Berridge, M. J. 1993. Inositol trisphosphate and calcium signaling. *Nature.* 361:315–325.

Boitano, S., E. R. Dirksen, and M. J. Sanderson. 1992. Intracellular propagation of calcium waves mediated by Inositol trisphosphate. *Science.* 258:292–295.

Bootman, M. D., and M. J. Berridge. 1995. The elemental principles of calcium signaling. *Cell.* 83:675–678.

Cuthberson, K. S. R., and T. R. Chay. 1991. Modeling receptor-controlled intracellular calcium oscillations. *Cell Calcium.* 12:97–109.

Dupont, G., and A. Goldbeter. 1994. Properties of intracellular $Ca^{2+}$ waves generated by a model based on $Ca^{2+}$-induced $Ca^{2+}$ release. *Biophys. J.* 67:2191–2204.

Eichwald, C., and F. Keiser. 1993. Model for receptor-controlled cytosolic calcium oscillations and for external influences on the signal pathway. *Biophys. J.* 65:2047–2058.

Friel, D. D. 1995. $[Ca^{2+}]_i$ oscillations in sympathetic neurons: an experimental test of a theoretical model. *Biophys. J.* 68:1752–1766.

Gold'shtein, V., and V. A. Sobolev. 1992. Qualitative analysis of singularly perturbed systems of chemical kinetics. *Am. Math. Soc. Transl.* 153:73–92.

Jacob, R. 1990. Agonist-stimulated divalent cation entry into single cultured human umbilical vein endothelial cells. *J. Physiol. (Lond.).* 421: 55–77.

Jafri, M. S. 1995. A theoretical study of cytosolic calcium waves in *Xenopus* oocytes. *J. Theor. Biol.* 172:209–216.

Jafri, M. S., and J. Keizer. 1995. On the roles of $Ca^{2+}$ diffusion, $Ca^{2+}$ buffers, and the endoplasmic reticulum in $IP_3$-induced $Ca^{2+}$ waves. *Biophys. J.* 69:2139–2153.

Kao, J. P. Y., and R. Y. Tsien. 1988. Ca binding kinetics of fura-2 and azo-1 from temperature-jump relaxation measurements. *Biophys. J.* 53: 635–639.

Keizer, J., and G. De Young. 1994. Simplification of a realistic model of $IP_3$-induced $Ca^{2+}$ oscillations. *J. Theor. Biol.* 166:431–442.

Kendall, J. M., R. L. Dormer, and A. K. Campbell. 1992. Targeting aequorin to the endoplasmic reticulum of living cells. *Biochem. Biophys. Res. Commun.* 187:1091–1097.

Korngreen, A., and Z. Priel. 1993. Signal transduction in ciliary systems: the effect of exogenous ATP on intracellular free calcium in human nasal epithelium. *Biophys. J.* 64:A76.

Korngreen, A., and Z. Priel. 1994. Simultaneous measurement of intracellular calcium and ciliary beating. *Biophys. J.* 67:377–380.

Korngreen, A., and Z. Priel. 1996. Purinergic stimulation of rabbit ciliated airway epithelia: control by multiple calcium sources. *J. Physiol. (Lond.).* 497:53–66.

Kraus, M., and B. Wolf. 1992. Mathematical model for agonist-induced oscillatory calcium waves in non-excitable mammalian cells. *Biol. Signals.* 1:101–113.

Lechleiter, J., S. Girard, E. Peralta, and D. Clapham. 1991. Spiral calcium wave propagation and annihilation in *Xenopus laevis* oocytes. *Science.* 252:123–126.

Levin, R., A. Braiman, and Z. Priel. 1997. Protein kinase C induced calcium influx and sustained enhancement of ciliary beating by extracellular ATP. *Cell Calcium.* 21:103–113.

Lückhoff, A., and D. E. Clapham. 1992. Inositol 1,3,4,5-tetrakisphosphate activates an endothelial $Ca^{2+}$-permeable channel. *Nature.* 355:356–358.

Mayer, T., and L. Stryer. 1988. Molecular model for receptor-stimulated calcium spiking. *Proc. Natl. Acad. Sci. USA.* 85:5051–5055.

Mitropol'skii, Yu. A., and O. B. Lykova. 1973. Integral Manifolds in Nonlinear Mechanics. Nauka, Moscow (in Russian).

Morgan, A. J., and R. Jacob. 1994. Ionomycin enhances $Ca^{2+}$ influx by stimulating store-regulated cation entry and not by a direct action at the plasma membrane. *Biochem. J.* 300:665–672.

Pozzan, T., R. Rizzuto, P. Volpe, and J. Meldolesi. 1994. Molecular and cellular physiology of intracellular calcium stores. *Physiol. Rev.* 74: 595–636.

Press, W. H., S. A. Teukolsky, W. T. Vetterling, and B. P. Flannery. 1992. Numerical Recipes in C, 2nd Ed. Cambridge University Press, New York.

Putney, J. W., Jr. 1990. Capacitative calcium entry revisited. *Cell Calcium.* 11:611–624.

Randriamampita, C., and R. Y. Tsien. 1993. Emptying of intracellular $Ca^{2+}$ stores releases a novel small messenger that stimulates $Ca^{2+}$ influx. *Nature.* 364:809–818.

Rasmussen, H., and J. E. Rasmussen. 1990. Calcium as intracellular messenger: from simplicity to complexity. *Curr. Top. Cell. Regul.* 31: 1–109.

Sneyd, J., J. Keizer, and M. J. Sanderson. 1995. Mechanism of calcium oscillations and waves: a quantitative analysis. *FASEB J.* 9:1463–1472.

Strygin, V. V., and V. A. Sobolev. 1988. Separation of Motion by the Method of Integral Manifolds. Nauka, Moscow (in Russian).

Takemura, H., A. R. Hughes, O. Thastrup, and J. W. Putney, Jr. 1989. Activation of calcium entry by the tumor promoter, thapsigargin, in parotid acinar cells. Evidence that an intracellular calcium pool, and not an Inositol phosphate, regulates calcium fluxes at the plasma membrane. *J. Biol. Chem.* 264:12266–12271.

Tang, Y., and H. G. Othmer. 1994. A model of calcium dynamics in cardiac myocytes based on the kinetics of ryanodine-sensitive calcium channels. *Biophys. J.* 67:2223–2235.

Tang, Y., and H. G. Othmer. 1995. Frequency encoding in excitable systems with applications to calcium oscillations. *Proc. Natl. Acad. Sci. USA.* 92:7869–7873.

Tarasiuk, A., M. Bar-Shimon, L. Gheber, A. Korngreen, Y. Grossman, and Z. Priel. 1995. Extracellular ATP induces hyperpolarization and motility stimulation of ciliary cells. *Biophys. J.* 68:1163–1169.

Tribe, R. M., M. L. Borin, and M. P. Blaustein. 1995. Functionally and spatially distinct $Ca^{2+}$ stores are revealed in cultured vascular smooth muscle cells. *Proc. Natl. Acad. Sci. USA.* 91:5908–5912.

Tsien, R. W., and R. Y. Tsien. 1990. Calcium channels, stores, and oscillations. *Annu. Rev. Cell Biol.* 6:715–60.

Wiesner, F. W., B. Berk, and R. M. Nerem. 1996. A mathematical model of cytosolic calcium dynamics in human umbilical vein endothelial cells. *Am. J. Physiol.* 270: C1556–C1569.

Zhou, Z., and E. Neher. 1993. Mobile and immobile calcium buffers in bovine adrenal chromaffin cells. *J. Physiol. (Lond.).* 469:245–273.